

## 12th June 2017 offshore Karaburun-Lesvos Island earthquake coseismic deformation analysis using continuous GPS and seismological data

Hasan YILDIZ<sup>1\*</sup>, Ayça ÇIRMIK<sup>2\*\*</sup>, Oya PAMUKÇU<sup>2</sup>, Özkan Cevdet ÖZDAĞ<sup>3</sup>, Tolga GÖNENÇ<sup>2</sup>,  
Muzaffer KAHVECİ<sup>4</sup>

<sup>1</sup>Higher Technical School of Surveying, General Directorate of Mapping, Ankara, Turkey

<sup>2</sup>Department of Geophysical Engineering, Faculty of Engineering, Dokuz Eylül University, İzmir, Turkey

<sup>3</sup>Earthquake Research and Implementation Center, Dokuz Eylül University, İzmir, Turkey

<sup>4</sup>Department of Surveying Engineering, Faculty of Engineering and Natural Sciences, Konya Technical University, Konya, Turkey

Received: 10.08.2020

Accepted/Published Online: 16.03.2021

Final Version: 17.05.2021

**Abstract:** Understanding the tectonic mechanism generated by the earthquakes and faults is possible only if the preseismic, coseismic and postseismic crustal deformation related to the earthquakes is determined properly. By the analysis of continuous GPS (CGPS) coordinate time series, it is possible to estimate the crustal deformation. Besides, accelerometer records at strong motion stations (SMSs) may support the CGPS-based estimates. In this study, CGPS coordinate time series were analyzed in comparison with the accelerometer records for clarifying the coseismic deformation caused by the earthquake occurred in the surrounding of Lesvos fault located in the northern part of Karaburun within the active mechanism that controls the area where the earthquakes occurred during June 2017 on the offshore Karaburun. The activity of this fault continued throughout June 2017 until the time when the main shock (12th June 2017,  $M_w = 6.2$ ) occurred. We analyzed CGPS coordinate time series of AYVL and CESM and DEUG stations to determine the coseismic deformation due to the offshore Karaburun-Lesvos Island earthquake using the empirical mode decomposition (EMD) method. Besides, the EMD method results were compared with the accelerometer records obtained from the SMSs close to the CGPS stations and CGPS-based results were found to be consistent with the accelerometer records. Additionally, the horizontal displacements were calculated by Coulomb 3.3 software using different focal plane solutions and compared with CGPS-based results. Consequently, it is suggested an integrated use of CGPS and strong motion accelerometer networks for the joint assessment of the crustal deformation and for the cost-effective use of existing observation networks as well as for the establishment of future observation networks at lower cost.

**Key words:** Lesvos Island, Karaburun, empirical mode decomposition (EMD), CGPS, accelerometer, horizontal-to-vertical spectral ratio (HVSr) curves

### 1. Introduction

The Aegean Sea is one of the most significant active seismic and deformation areas in Anatolian, Eurasian and African tectonic plates. This region is affected by the strike-slip tectonic regime which is the general characteristic of the North Anatolian Fault Zone (NAFZ) and by the extension regime of Western Anatolia. Due to these tectonic features, there have been severe earthquakes in this area both in the historical and instrumental period.

The Northern Aegean region is a complex tectonic region of the Anatolian plate moving towards west along the North Anatolian Fault. This region is under the effect of the interaction of North Aegean Trough (NAT) and Western Anatolian graben system (WAGS) (Papazachos and Kiratzi, 1996; Kiratzi and Louvari, 2003; Pavlides et al., 2009) (Figure 1a). The interaction of NAT and WAGS

causes different fault character and trending in this region (Koukouvelas and Aydin, 2002; Kreemer et al., 2004; Papanikolaou et al., 2006). These faults are observed along small islands and seafloor morphology. The Lesvos Island, located in the seismological active Aegean Sea, presents intensive seismic activity. Lesvos Island includes E-W and approximately N-S trending multiple fault structures (Figure 1b). A structural discontinuity, Aghia-Paraskevi fault (APF) with 17 km length is located along NE-SW direction in the midregion of the island and continues under the Kalloni Gulf having the maximum earthquake potential (Pavlides et al., 2009).

During the period from 1979 to 2017 five main shocks ( $4 \leq M \leq 6.2$ ) occurred to the south of the Lesvos Island close to the Polichnitos-Plomari and Aghios Isidoros-Cape Magiras faults (Figure 1b) at the Lesvos fault system. These

\* Correspondence: ayca.cirmik@deu.edu.tr

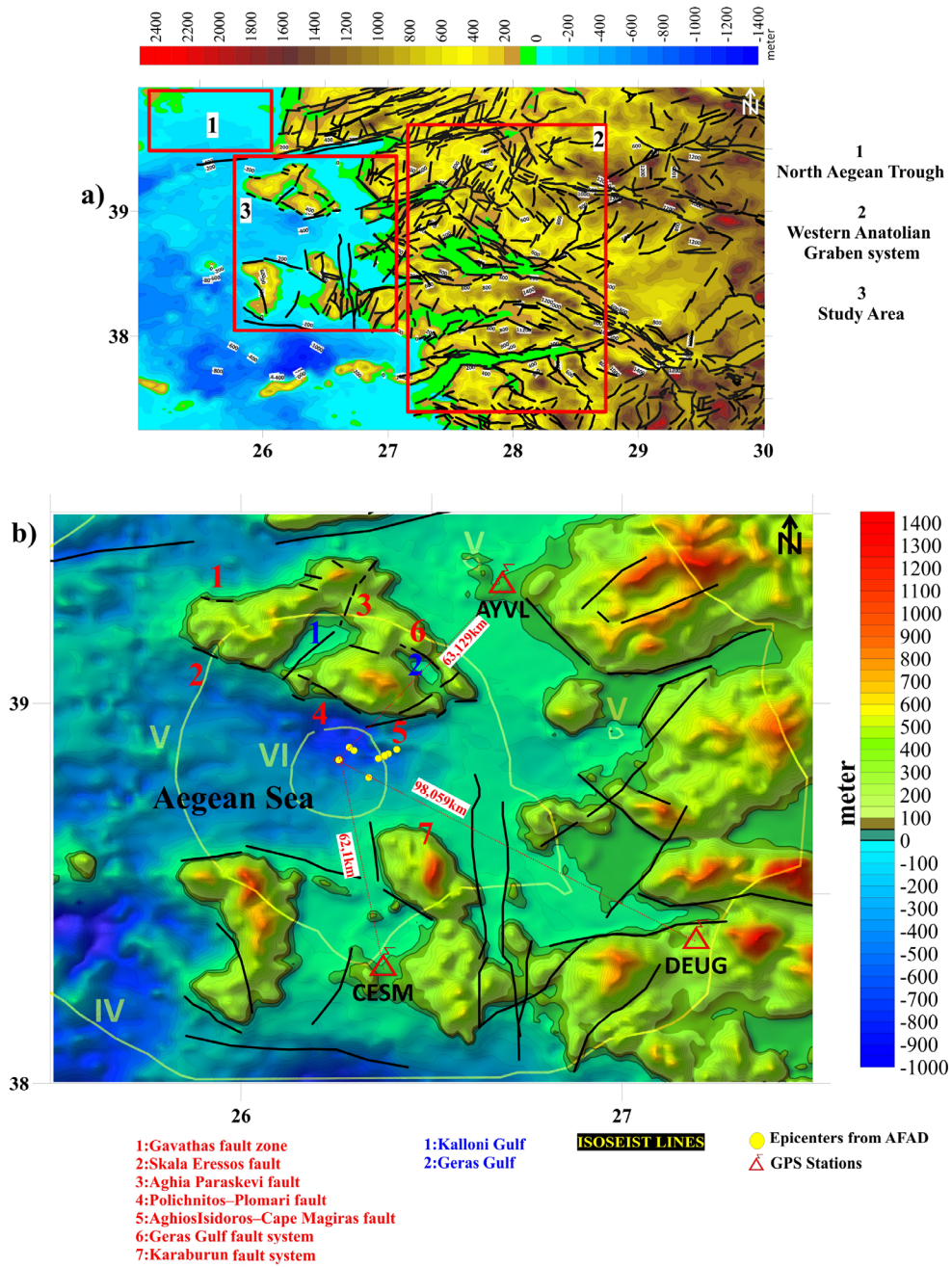


**Figure 1.** a) The main tectonic elements of the study region and its surroundings (Pavlidis et al., 2009; Chatzipetros et al., 2013). Faults (Zouros et al., 2011; modified from Sözbilir et al., 2017)<sup>1</sup> are shown with black lines. b) The locations of the accelerometers and CGPS stations with respect to the epicentre of 12th June 2017 Earthquake. The isoseist lines show the earthquake intensity (map modified from KOERI, 2017)<sup>2</sup>. The intensity for the AVVL and CESH stations are between IV and V, and IV for the DEUG station. The yellow dots represent the earthquakes occurred at 12th June 2017 (obtained from AFAD, 2017)<sup>23</sup>.

<sup>1</sup>Sözbilir H, Sümer Ö, Uzel B, Eski S, Tepe Ç et al. (2017). 12 Haziran 2017 Midilli Depremi (Karaburun Açıkları) ve Bölgenin Depremselliği, Dokuz Eylül Üniversitesi Deprem Araştırma ve Uygulama Merkezi Diri Fay Araştırma Grubu [online]. Website <http://daum.deu.edu.tr/wp-content/uploads/2019/07/Midilli-Deprem-Raporu.pdf> [accessed 01 March 2021] (in Turkish).

<sup>2</sup>KOERI (Kandilli Observatory and Earthquake Research Center) (2017). 12 Haziran 2017 Karaburun Açıkları-Ege Denizi Depremi [online]. Website [http://www.koeri.boun.edu.tr/sismo/2/wp-content/uploads/2017/06/12\\_HAZIRAN\\_2017\\_EGE\\_DENIZI\\_DEPREMI.pdf](http://www.koeri.boun.edu.tr/sismo/2/wp-content/uploads/2017/06/12_HAZIRAN_2017_EGE_DENIZI_DEPREMI.pdf) [accessed 01 March 2021] (in Turkish).

<sup>3</sup>AFAD (The Disaster and Emergency Management Presidency of Turkey) (2017). 12 Haziran 2017 Ege Denizi Depremi (Karaburun Açıkları) Ön Değerlendirme Raporu [online]. Website <https://deprem.afad.gov.tr/depremkatalogu> [accessed 01 March 2021] (in Turkish).

nearly E-W trending faults are located perpendicular to the Karaburun fault system (Figure 1b). Besides, NW-SE trending Polichnitos-Plomari fault has thermal activity due to the Polichnitos geothermal field (Günther et al., 1977). WSW-ENE trending Aghios Isidoros-Cape Magiras fault extends along the SE border of the Lesvos Island.

The offshore Karaburun-Lesvos Island earthquake (Figures 1b and 2) occurred on 12th June 2017 and affected a wide region (Figure 1b) (Briole et al., 2018; Papadimitriou et al., 2018). The magnitude of this earthquake is  $M_w = 6.2$  according to Kandilli Observatory and Earthquake Research Center (KOERI, 2017)<sup>1</sup> and Disaster and Emergency Management Presidency of Turkey (AFAD, 2017)<sup>2</sup>,  $M_w = 6.3$  according to U.S. Geological Survey (USGS 2017)<sup>3</sup>. The hypocenter of the earthquake is 6.96 km. Additionally, eight aftershocks ( $M \geq 4$ ) occurred after the main shock ( $M = 6.2$ ) on 12th June 2017 near to the Lesvos Island (Figure 2, Table 1).

In this study, 12th June 2017 offshore Karaburun-Lesvos Island earthquake (Figures 1b and 2) coseismic deformation analysis was carried out applying the empirical mode decomposition (EMD) method to the coordinate time series of three CGPS stations namely AYVL (Ayvalık, Balıkesir City) (Figure 3a), CEM (Çeşme, İzmir city)

(Figure 3b) and DEUG (Dokuz Eylül University, İzmir city) (Figure 3c).

The EMD method was developed for separating the nonlinear and nonstationary time series into a certain number of single component signals (Huang et al., 1998). It is considered that the EMD method is suitable for separating the CGPS coordinate time series into single component signals. CGPS coordinate the time series include interseismic linear trend and periodic signals such as annual and semiannual signals and noise. In addition to these signals, CGPS time series include coseismic offsets if affected by an earthquake. Initially, to test the performance of the EMD method for the removal of periodic signals and noise and for the detection of the offsets, synthetic time series were constructed like a typical CGPS coordinate time series affected by an earthquake. Subsequently, the EMD method was applied to three CGPS coordinate time series in Western Anatolia to estimate the coseismic deformation generated by 12th June 2017 offshore Karaburun-Lesvos Island Earthquake.

Additionally, horizontal-to-vertical spectral ratio (HVSr) curves are calculated using the Nakamura method (Nakamura, 1989) for the strong motion station (SMS) of AFAD which are close to CGPS stations by using the horizontal and vertical components of 12th June 2017

<sup>1</sup>KOERI (Kandilli Observatory and Earthquake Research Center) (2017). 12 Haziran 2017 Karaburun Açıkları-Ege Denizi Depremi [online]. Website [http://www.koeri.boun.edu.tr/sismo/2/wp/content/uploads/2017/06/12\\_HAZIRAN\\_2017\\_EGE\\_DENIZI\\_DEPREMI.pdf](http://www.koeri.boun.edu.tr/sismo/2/wp/content/uploads/2017/06/12_HAZIRAN_2017_EGE_DENIZI_DEPREMI.pdf) [accessed 01 March 2021] (in Turkish).

<sup>2</sup>AFAD (The Disaster and Emergency Management Presidency of Turkey) (2017). 12 Haziran 2017 Ege Denizi Depremi (Karaburun Açıkları) Ön Değerlendirme Raporu [online]. Website <https://deprem.afad.gov.tr/depremkatalogu> [accessed 01 March 2021] (in Turkish).

<sup>3</sup>U.S. Geological Survey (2017). Earthquakes event page [online] Website <https://earthquake.usgs.gov/earthquakes/eventpage/us20009ly0/moment-tensor> [accessed 17 03 2021].

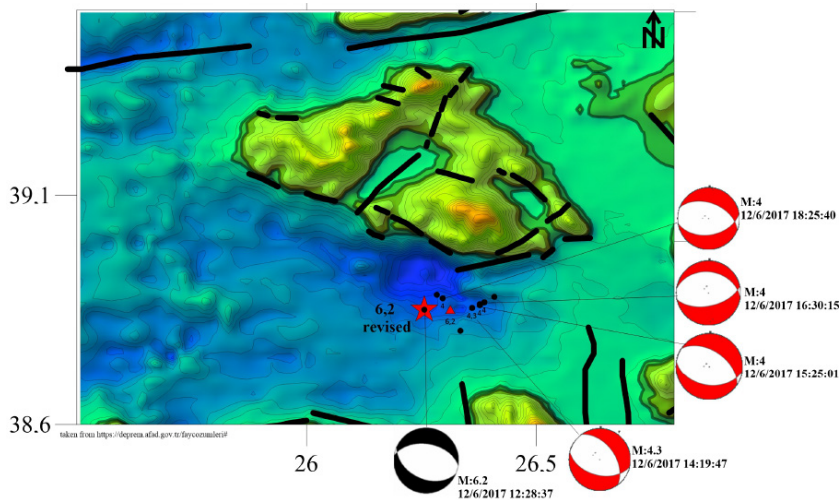


**Figure 2.** The view of the epicentres and the focal mechanisms of the earthquakes occurred on 12th June 2017. The red star and red triangles represent the revised epicentre and the first announced epicentre of the main shock, respectively. The black dots represent the aftershocks occurred on 12th June 2017 (obtained from AFAD, 2017)<sup>2</sup>. The black lines represent the faults in the Lesvos Island (Zouros et al., 2011; modified from Sözbilir et al., 2017<sup>4</sup>).

**Table 1.** The list of the main shock and the aftershocks ( $M \geq 4$ ) occurred on 12th June 2020 (obtained from AFAD).

Date	Time	Latitude (°)	Longitude (°)	Depth (km)	Magnitude	Magnitude type
12/06/2017	12:28:37	38.8511	26.2565	6.96	6.2	M <sub>w</sub>
12/06/2017	12:31:39	38.8840	26.2835	7.00	4.9	M <sub>w</sub>
12/06/2017	12:32:54	38.8051	26.3345	7.02	4.0	M <sub>L</sub>
12/06/2017	12:35:33	38.8630	26.3766	4.78	4.9	M <sub>w</sub>
12/06/2017	12:47:25	38.8790	26.4085	7.05	4.5	M <sub>w</sub>
12/06/2017	14:19:47	38.8548	26.3601	12.42	4.3	M <sub>w</sub>
12/06/2017	15:25:01	38.8608	26.3770	6.97	4.0	M <sub>w</sub>
12/06/2017	16:30:15	38.8673	26.3866	12.29	4.0	M <sub>w</sub>
12/06/2017	18:25:40	38.8760	26.2961	12.53	4.0	M <sub>w</sub>



(a)

(b)



(c)

**Figure 3.** The views of CGPS stations used in this study. a) The view of AYVL station located in Ayvalık (Balıkesir city). b) The view of CESM station located in Çeşme (İzmir city). c) The view of the DEUG station located in Dokuz Eylül University, Tınaztepe Campus, İzmir.

Earthquake accelerometer records and the CGPS-based estimates were compared with accelerometer records. Besides, the offsets in the CGPS time series estimated by the EMD method were evaluated with the displacements calculated by the Coulomb 3.3 software (Toda et al., 2011).

## 2. GPS data processing

GPS data collected at three CGPS stations (AYVL, CESH and DEUG) (Figures 1b and 3) located in Western Anatolia near to the Lesvos Island and to the epicenter of the 12th June 2017 offshore Karaburun-Lesvos Island earthquake were processed. AYVL and CESH are the continuous stations of the Continuously Operating Reference Stations-Turkey (CORS-TR) and DEUG station was built in Dokuz Eylül University, Tinaztepe Campus within the Dokuz Eylül University Scientific Research Project (No: DEU 2015.KB.FEN.034) collecting data since October 2016. For the investigation of earthquake coseismic deformation approximately five months (153 days) GPS data for the period from 1st April (91th day as Julian day) to 1st September (243rd day as Julian day) were processed and CGPS coordinate time series were obtained by using Gamit/Globk software (Herring et al., 2015). In this processing, 9 IGS stations (BUCU, GLSV, ISTA, MATE,

MIKL, NICO, PENC, TUBI and ZECK) (Figure 4) were used for the realization of Eurasian fixed reference frame. The GPS processing strategy is given at Table 2.

Due to the very high weighted rms (wrms) values of the time series of AYVL station caused by large spikes on 25th June 2017 (176th Julian day) and 21st July 2017 (202nd Julian day), solutions of these two daily solutions were removed from the AYVL CGPS time series.

## 3. Empirical mode decomposition (EMD) method and its application on the synthetic time series

The EMD method developed by Huang et al. (1998) decomposes a time series into a finite number of amplitude and frequency modulated components referred to as intrinsic mode functions (IMF). It is a posterior method in which the decomposition adapts to and is derived directly from the data. The EMD method can be applied to nonstationary and nonlinear data. The method works by identifying the different time-scales in the data and separating these into individual IMFs that are found iteratively by sifting algorithm (Huang et al., 1998; Rato et al., 2008). After applying the sifting process, the first IMF corresponding to the highest frequencies in the original signal is determined (Baykut et al., 2010). Once the first

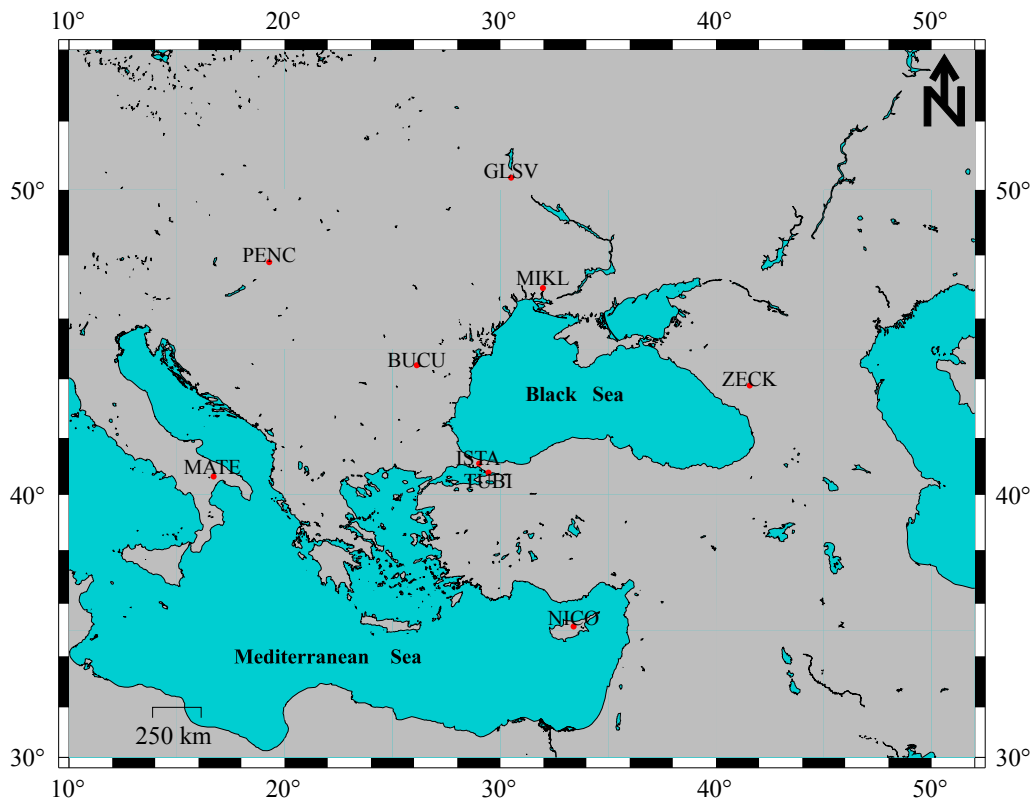


**Figure 4.** The distribution of the IGS stations used for Eurasian fixed reference frame realization. This map was created by using GMT software (Wessel et al., 2019).

IMF has been obtained, it is subtracted from the original data producing residuals. The residuals are subjected to the same process, yielding the second IMF and so on, until satisfying a stopping criteria (Rato et al., 2008) and a final residual (last IMF), which generally corresponds to lowest frequency in the original signal is obtained. The EMD method has been previously applied for the time series analysis of atmosphere, climate, oceanography (Huang and Wu, 2008), seismic data (Huang et al., 2001), soil radon data (Baykut et al., 2010) and for denoising CGPS coordinate time series (Baykut et al., 2009). In this study the EMD code developed by Rato et al. (2008) was used.

The performance of the EMD method was tested by applying the method to a synthetic daily coordinate time series generated by intercept and site velocity terms, annual, semiannual signals and a step function with an offset simulating a coseismic offset associated with an earthquake and adding white and flicker noise (Mao et al., 1999; Williams et al., 2004). The length of the time series is 153 days as the length of the CGPS daily coordinate time series used in this study.

The parameters used in this study are presented in Table 3 to create the synthetic coordinate time series (Figure 5) by using the formula:

$$s(t) = x_0 + vt + \sum_{k=1}^2 A_k \cos[2\pi f_k(t) + \phi_k(t)] + O(t) + e(t), \quad (1)$$

where  $x_0$  and  $v$  are intercept and site velocity terms, and  $A_k$  are the amplitude, frequency and phase angles of annual and semiannual signals,  $O(t)$  is step function representing the offset;

$$O(t) = \begin{cases} 0 & t_i > t_j \\ 1 & t_i < t_j \end{cases}$$

and  $e(t)$  is the combination of white and flicker noise. The different signal components of synthetic daily time series are shown on Figure 6.

The synthetic signal was separated into the six IMFs (IMFS 1-6) (Figures 7a–7f) by the EMD method. Results showed that the IMF-1 (Figure 7a) seems to include noise signals whereas the IMF-2 (Figure 7b) and IMF-3 (Figure 7c) represent periodic oscillations. The last IMF

**Table 2.** GPS data processing strategy.

Software	Gamit/Globk Version 10.61
Sampling of the GPS data	30 s/ 24 h daily data
Processing days	1st April – 1st September 2017 (91st – 243rd Julian days)
Cut-off angle	10°
Ephemeris information	IGS final orbits and IGS ERP files
Antenna phase center information	Weighted phase center model related to the height angle (PCV-antmod.dat)
Troposphere parameter	VMF1 (Vienna Mapping Function) were used. Zenith delay parameters were calculated for every 2 h.
International Terrestrial Reference System	ITRF 2008
Fixed stations	Eurasian fixed reference frame was chosen. BUCU, GLSV, ISTA, MATE, MIKL, NICO, PENC, TUBI and ZECK were used as reference.
Final coordinate computation	153 daily GPS data were combined with Globk.

**Table 3.** The parameters used to create the synthetic daily coordinate time series.

Parameter	Amplitude	Variance
Annual signal (mm)	2	-
Semiannual signal (mm)	1	-
Intercept term (mm)	10	-
Site velocity (mm/year)	2	-
Offset (mm)	5	-
White noise (mm)	-	1
Flicker noise (mm/year <sup>1/4</sup> )	-	1

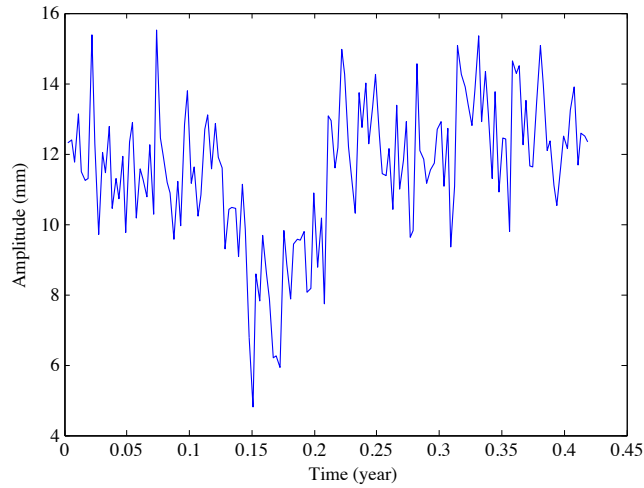


Figure 5. Synthetic daily coordinate time series.

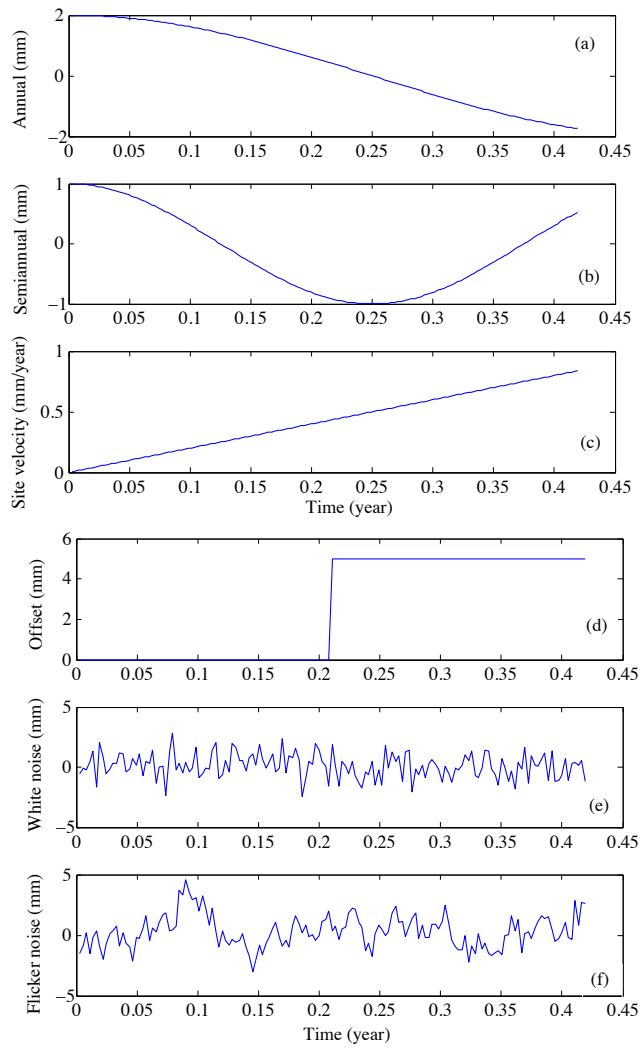
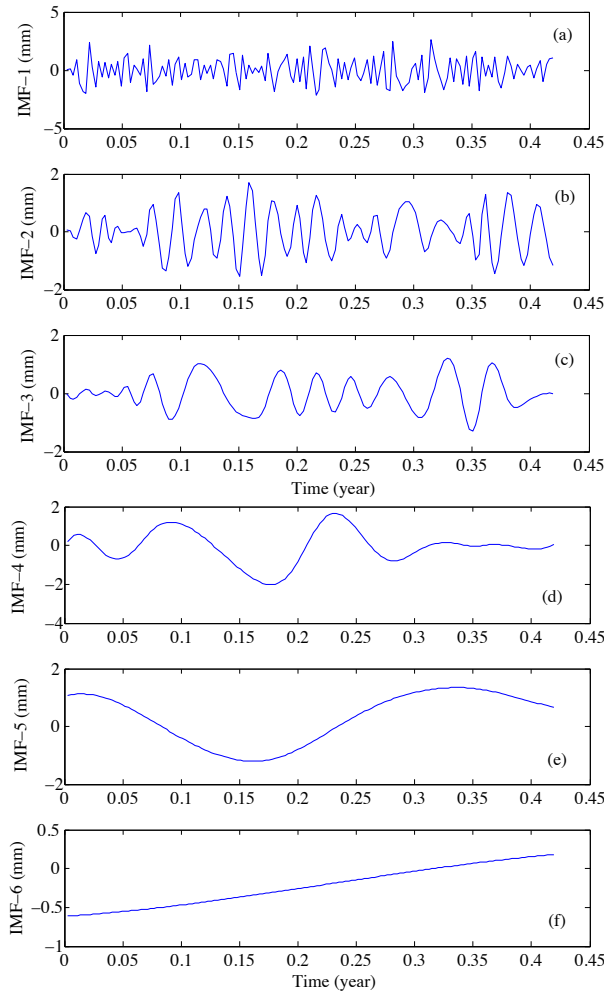
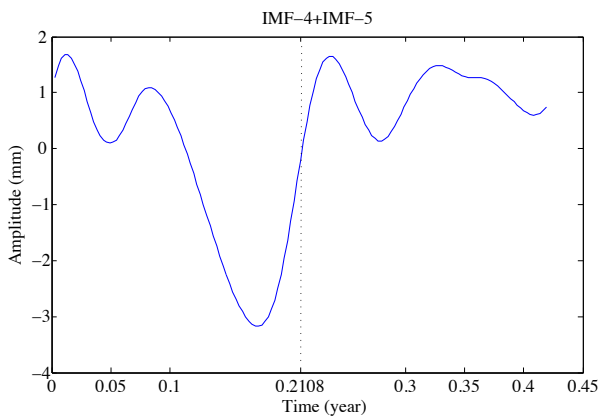


Figure 6. Components of synthetic daily time series. a) annual signal, b) semiannual signal, c) site velocity, d) step functions simulating a coseismic offset associated with an earthquake, e) white noise, f) flicker noise.



**Figure 7.** Intrinsic mode functions (IMF1-6 Figures 7a and 7f).



**Figure 8.** Summation of the IMF-4 and IMF-5 (IMF-4 + IMF-5) results in an offset signal with approximately same occurrence time and amplitude as the input offset signal in synthetic time series. The offset occurrence time is plotted with black dotted line.

mode (IMF-6) (Figure 7f), corresponding to the longest wavelength signal, represents the synthetically generated site velocity. The summation of the IMF-4 (Figure 7d) and IMF-5 (Figure 7e) approximately represents the synthetically generated offset signal.

By the summation of the IMF-4 and IMF-5, (IMF-4+IMF-5), the offset signal approximately at the offset occurrence time and approximately at the same amplitude as the input offset signal in the synthetic time series could be obtained (Figure 8).

**4. EMD analysis of CGPS time series for the deformation analysis for 12th June 2017 offshore Karaburun-Lesvos Island earthquake**

Numerous faults were defined by Pavlides et al. (2009) and Chatzipetros et al. (2013) in the southern margin of the Lesvos Island where the 12th June 2017 offshore Karaburun-Lesvos Island earthquake occurred. The deformation

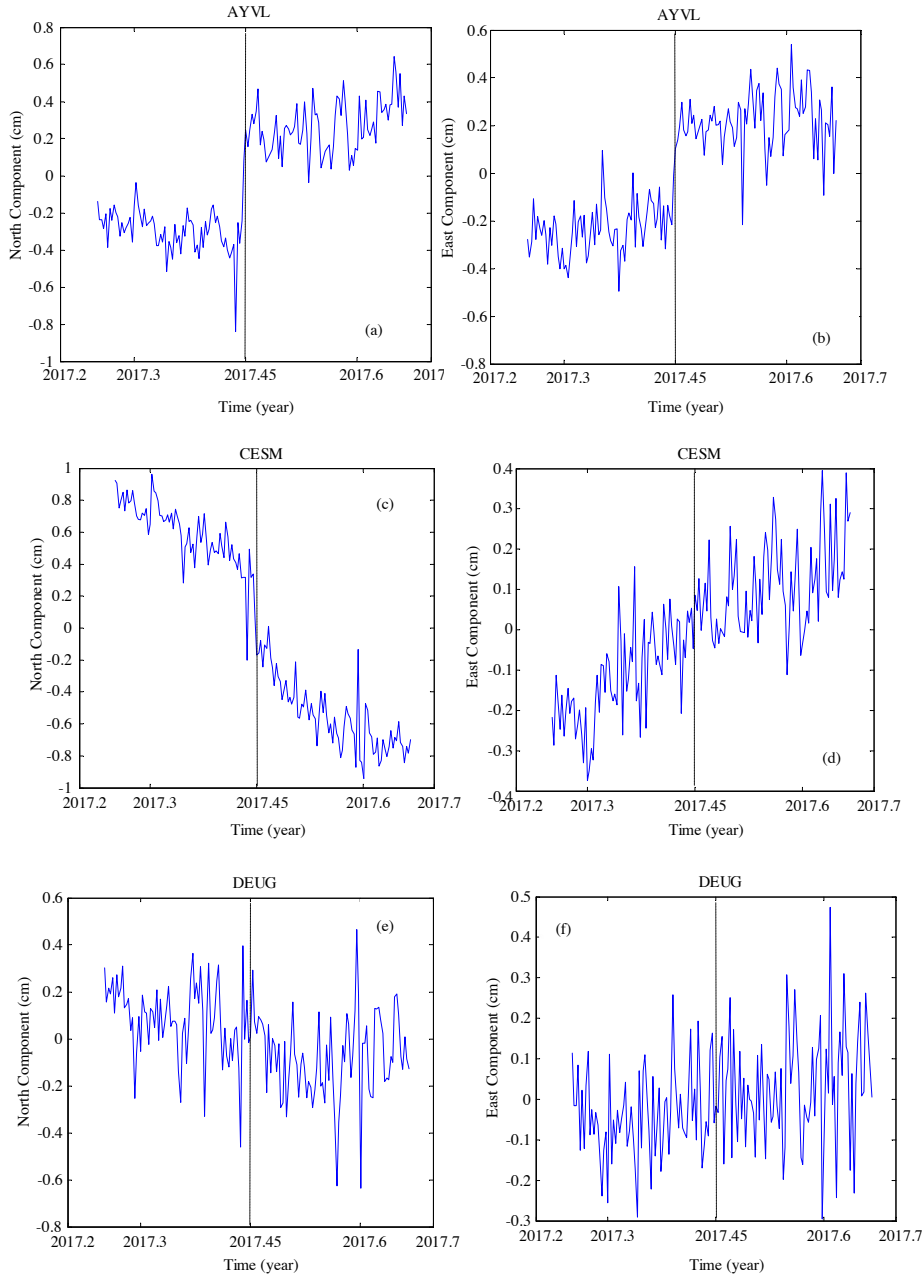


**Figure 9.** North and East components of time series of AYVL (a, b), CESH (c, d) and DEUG (e, f) stations. Earthquake occurrence time is plotted with black dotted line.

zone in the south of the Lesvos Island may be characterized by a steeply graded, stepped geometry, containing a small amount of lateral component and sloping normal faulting. To reveal the coseismic deformation on the Western Anatolia generated by this earthquake, three CGPS stations in Turkey, AYVL, CESH and DEUG were used. The distances of these CGPS stations to the earthquake epicenter are shown in Figure 1b.

The North and East components of CGPS coordinate time series of AYVL (Figures 9a and 9b), CESH (Figures 9c and 9d) and DEUG (Figures 9e and 9f) are shown. Any coseismic signal is not noticed in the vertical (Up) component of these 3 CGPS stations; therefore, neither the original CGPS Up component of the time series nor the IMFs of the Up component of the time series are shown. By the way, the results only for horizontal

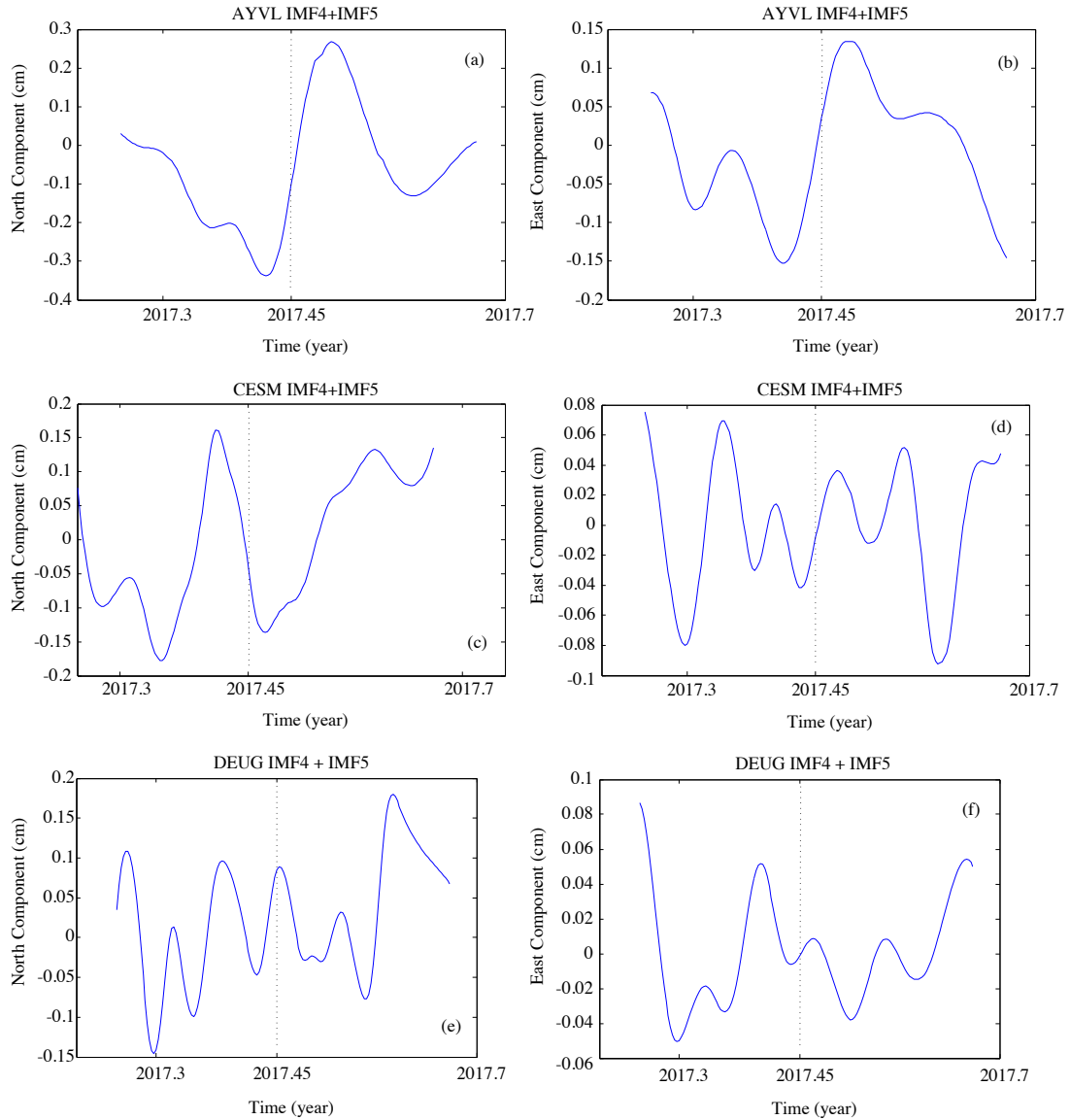


**Figure 10.** a) The summation of IMF-4 and IMF-5 modes for North component, b) East component of the coordinate time series of AYVL, c) the summation of IMF-4 and IMF-5 modes for North component, d) East component of the coordinate time series of CESM, e) the summation of IMF-4 and IMF-5 modes for North component, f) East component of the coordinate time series of DEUG. Earthquake occurrence time is plotted with black dotted line.

components (North and East) were given. The North and East components of the time series of AYVL, CESM and DEUG stations are separated into different IMFs by the EMD method. Consequently, using the summation of the IMF-4 and IMF-5, the coseismic offset signals are aimed to be determined (Figure 10).

##### 5. Accelerometer records of strong motion stations (SMSs)

As it is well known, the earthquake waves originating from the earthquake source travel through the bedrock

and reach the soil by passing to the soil layers. Along this route, the frequency and amplitude of the earthquake waves vary depending on the medium in which they pass through. These variations are evaluated in terms of linear system theory (Kramer, 1996). The linear system (Figure 11) is used for calculating the variations on the earthquake waves along the ray paths (Figure 12).

Nakamura (1989) method is based on the assumption that there is a parallelism between the small vibrations forming in the ground for various reasons and surface waves. By this method, HVSR is calculated dividing the

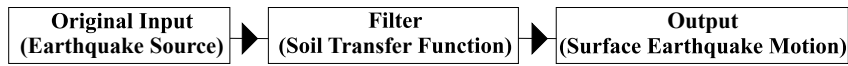


Figure 11. The flow chart of the linear system.

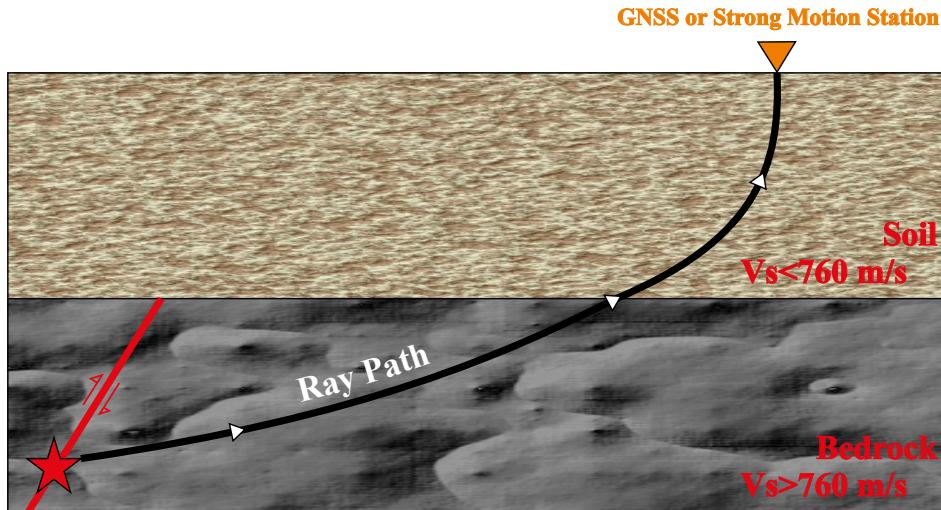


Figure 12. Schematic distribution of the ray path of the earthquake from the hypocenter to the ground surface.

spectrum of the horizontal components by the spectrum of the vertical component of the microtremors or accelerometers. The HVSr is a function of the frequency that will produce the horizontal/vertical (H/V) curves corresponding to the soil transfer function (Figure 12).

Soil transfer functions define the effects of layers between bedrock and soil on earthquake waves. These functions can be calculated theoretically using the physical properties of the layers between bedrock and soil, or on site using the HVSr curves calculated by the Nakamura method. The general overview, historical development and various applications of the HVSr method are given in Mucciarelli and Gallipoli (2001) in detail.

The North (N), East (E) and Up (Z) components of 12th June 2017 Earthquake accelerometer records (Figures 13–15, respectively) obtained from the SMSs of AFAD close to the CGPS stations (Figure 1b), namely, AYVL (Ayvalık SMS near to AYVL CGPS station); CESM (Çeşme SMS near to CESM CGPS station), TNZB (Dokuz Eylül University Tinaztepe Campus SMS near to DEUG CGPS station) are used to compute the HVSr curves (Figure 16) by the Nakamura method to determine the soil behaviour of the station locations affected by the earthquake (Nakamura, 1989).

## 6. Discussion

The EMD analysis of the north and east components of three CGPS stations (AYVL, CESM and DEUG) are

presented in Figure 10. The coseismic offsets of the North and East components of AYVL station are approximately 0.6 cm and 0.3 cm, respectively (Figures 10a and 10b). The coseismic offset of the North component of the CESM station is approximately –0.3 cm (Figure 10c) whereas the East component shows almost no offset (Figure 10d). Also, no coseismic offsets are detected in the DEUG CGPS time series (Figures 10e and 10f).

The investigation of the accelerometer records of AYVL (Figure 13) and CESM SMSs (Figure 14) suggest the larger N-S and E-W amplitudes with respect to Z component. Besides, TNZB SMS (Figure 15) shows much smaller amplitudes than AYVL and CESM SMSs indicating that the TNZB SMS is less affected by the earthquake which is in agreement with CGPS-based coseismic estimates of DEUG CGPS station shown on Figures 9e and 9f and earthquake intensity map (Figure 1b). The HVSr curves (Figure 16) were calculated using the 12.06.2017 ( $M_w = 6.2$ ) Earthquake accelerometer records of AYVL (Figure 13), CESM (Figure 14) and TNZB (Figure 15) SMSs.

Although some minor differences are observed, the local site effects (from HVSr curves) of AYVL and CESM stations (Figure 16a) are generally similar. It is evidenced by the fact that the PGA values of the SMSs are very close to each other. If the local ground conditions of AYVL and CESM stations were different, it would be expected that there would be large differences in the PGA values they would record due to the difference in ground amplification

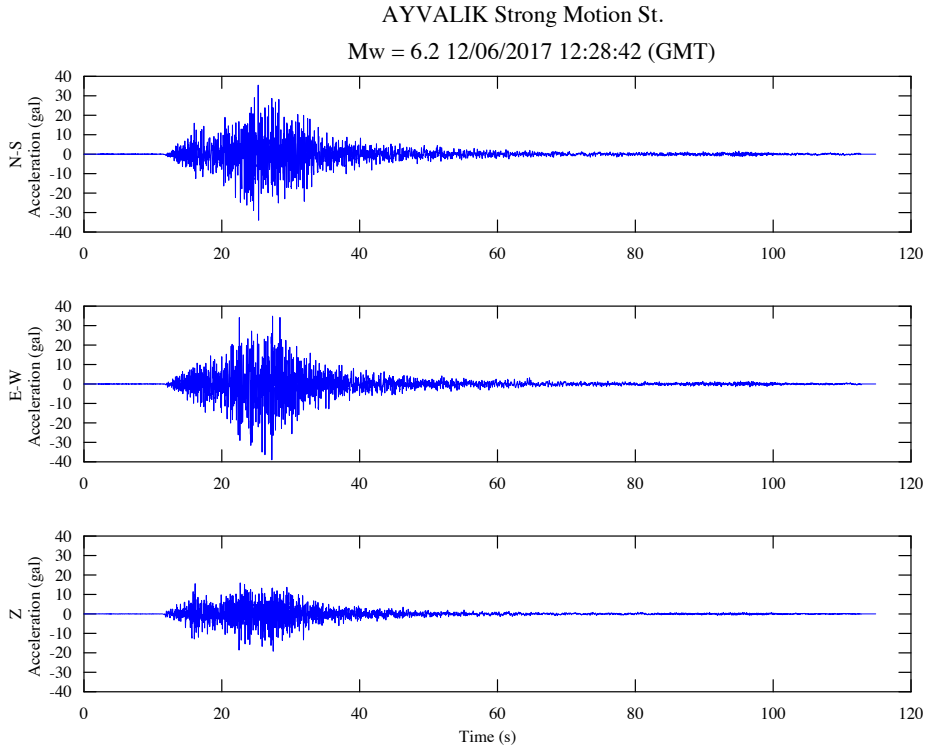


**Figure 13.** The 12th June 2017 Earthquake accelerometer record of Ayvalık strong motion station (AYVL SMS).

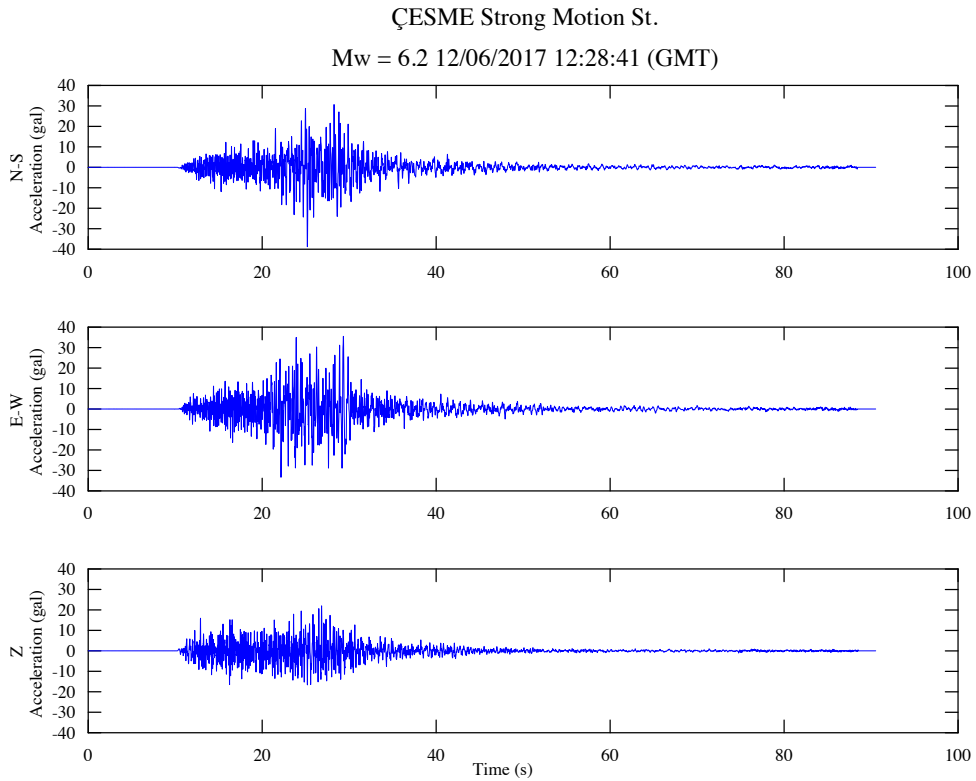


**Figure 14.** The 12<sup>th</sup> June 2017 Earthquake accelerometer record of Çeşme strong motion station (CESM SMS).

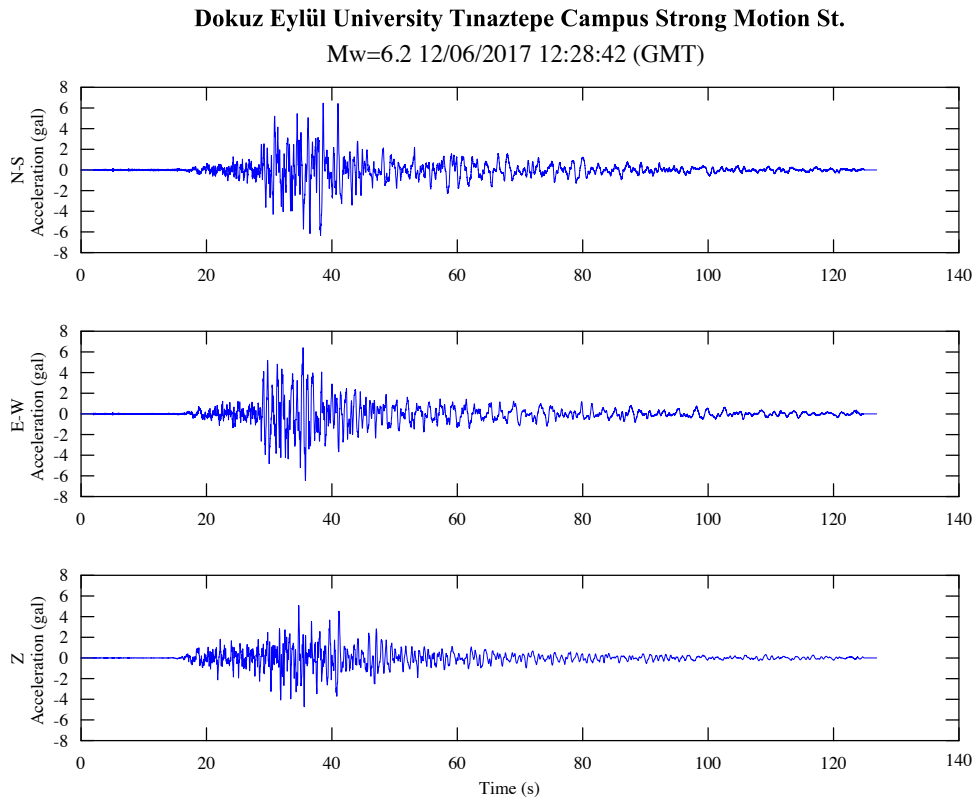


**Figure 15.** The 12th June 2017 Earthquake record of Dokuz Eylül University Tınaztepe Campus Strong Motion Station (TNZB SMS).

(AYVL= -38.899899 Gal, CESM= -38.8805939 Gal). On the other hand, TNZB SMS recorded smaller acceleration values (Figure 15) during the earthquake due to its distance from the epicenter and the difference of its local site effects (Figure 16b). The TNZB SMS (Figure 15) suggests a lower PGA value (TNZB = 6.472011 Gal) than the other two stations indicating that TNZB station shows a totally different character (local site effects) than AYVL and CESM stations. Therefore, the Nakamura method (Figure 16) suggest that AYVL and CESM SMSs present nearly similar character with each other, but TNZB station shows a totally different character (local site effects) than AYVL and CESM accelerometers. These results are consistent with the EMD analysis results of CGPS stations (AYVL, CESM and DEUG).

To evaluate the CGPS-based offsets, the Coulomb 3.3 software (Toda et al., 2011) was used to compute the horizontal displacements (Figure 17). In this calculation, the horizontal displacements were obtained by using the fault plane solutions of USGS (2017)<sup>3</sup>, Papadimitriou et al. (2018), KOERI (2017)<sup>1</sup> and AFAD (2017)<sup>2</sup> (Table 4) for the 12th June 2017 offshore Karaburun-Lesvos Island earthquake. In this calculation, it is assumed that the model is a half-space elastic medium. The Young's modulus (E),

Poisson's ratio and friction coefficient ( $\mu$ ) were used as  $8E+05$  bar, 0.25 and 0.4, respectively. The values of the horizontal displacements are given at Table 5 and the horizontal displacements for the focal plane solutions of USGS are shown in Figure 17.

The horizontal displacements calculated by Coulomb 3.3 software using source parameters computed by different institutions generally agree with each other. The modelled horizontal displacements and the offsets in CGPS time series agree with each other except the east component of CESM station (Table 4). The earthquake waves during the global spreading are affected by the rheological structure, discontinuities and the presence of fluid in an underground formation, so these factors affect the amplitudes and the directions of the earthquake waves. Besides, in the horizontal displacement calculation, the medium, which controls the environmental propagation of the earthquake source's impact, is assumed uniform. However, the offsets detected from CGPS time series at the medium where the earthquake waves were affected by the rheological structures, in the other words, the medium is heterogeneous in this calculation. Therefore, the mentioned effects may be the reason of the misfit between the results.

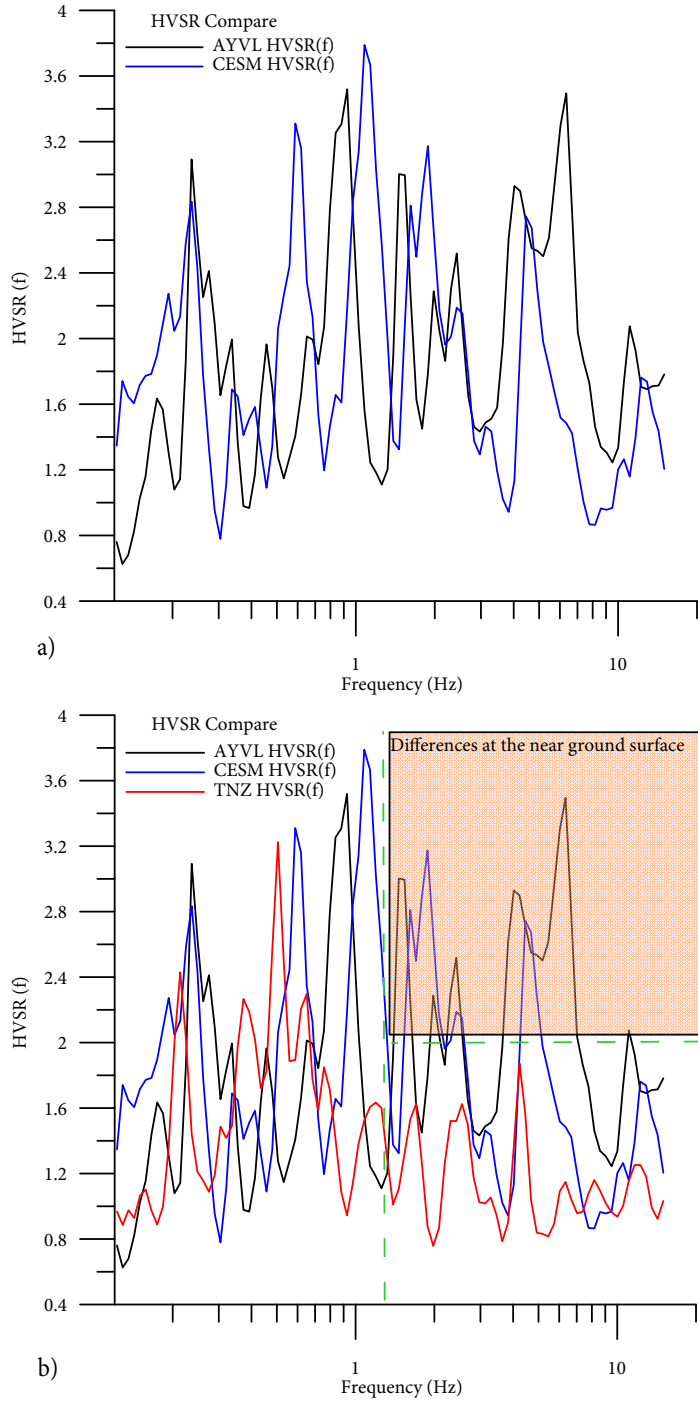


**Figure 16.** HVSR curves of a) AYVL, CESH SMSs, b) AYVL, CESH and TNZB SMSs.

Additionally, when the results of the Nakamura method are considered, it is observed that the soil characteristics of AYVL and CESH SMSs present minor differences. AYVL, CESH and TNZB (very close to the DEUG CGPS station) are located at Neogene volcano-sedimentary basins (Figure

18), however, the tectonic mechanism which controls the stations are different. While AYVL and CESH stations are located in the west of the İzmir-Balıkesir Transform Zone (Sözbilir et al., 2011), TNZB is located inside this zone (Figure 18). Therefore, the tectonism related with

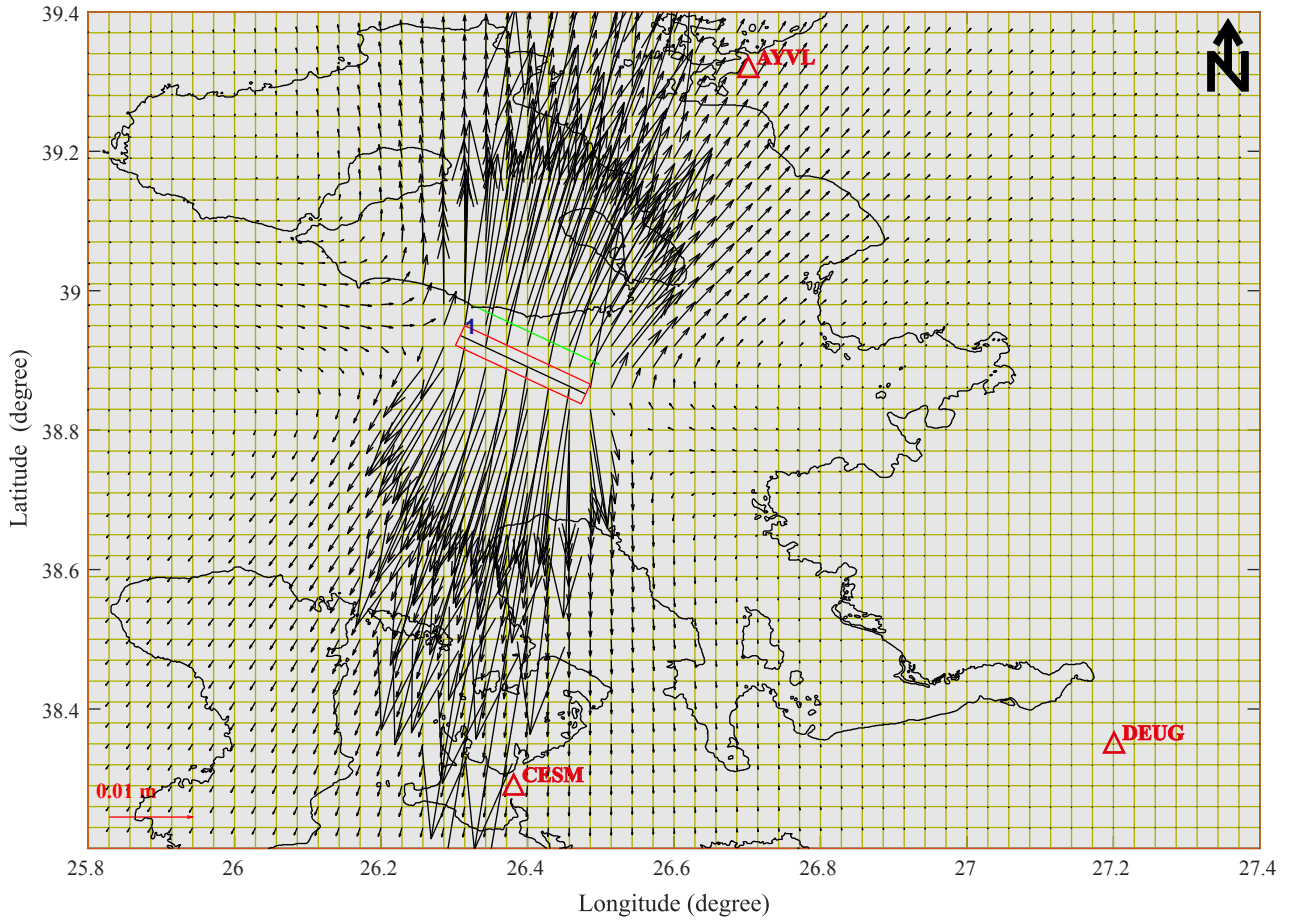


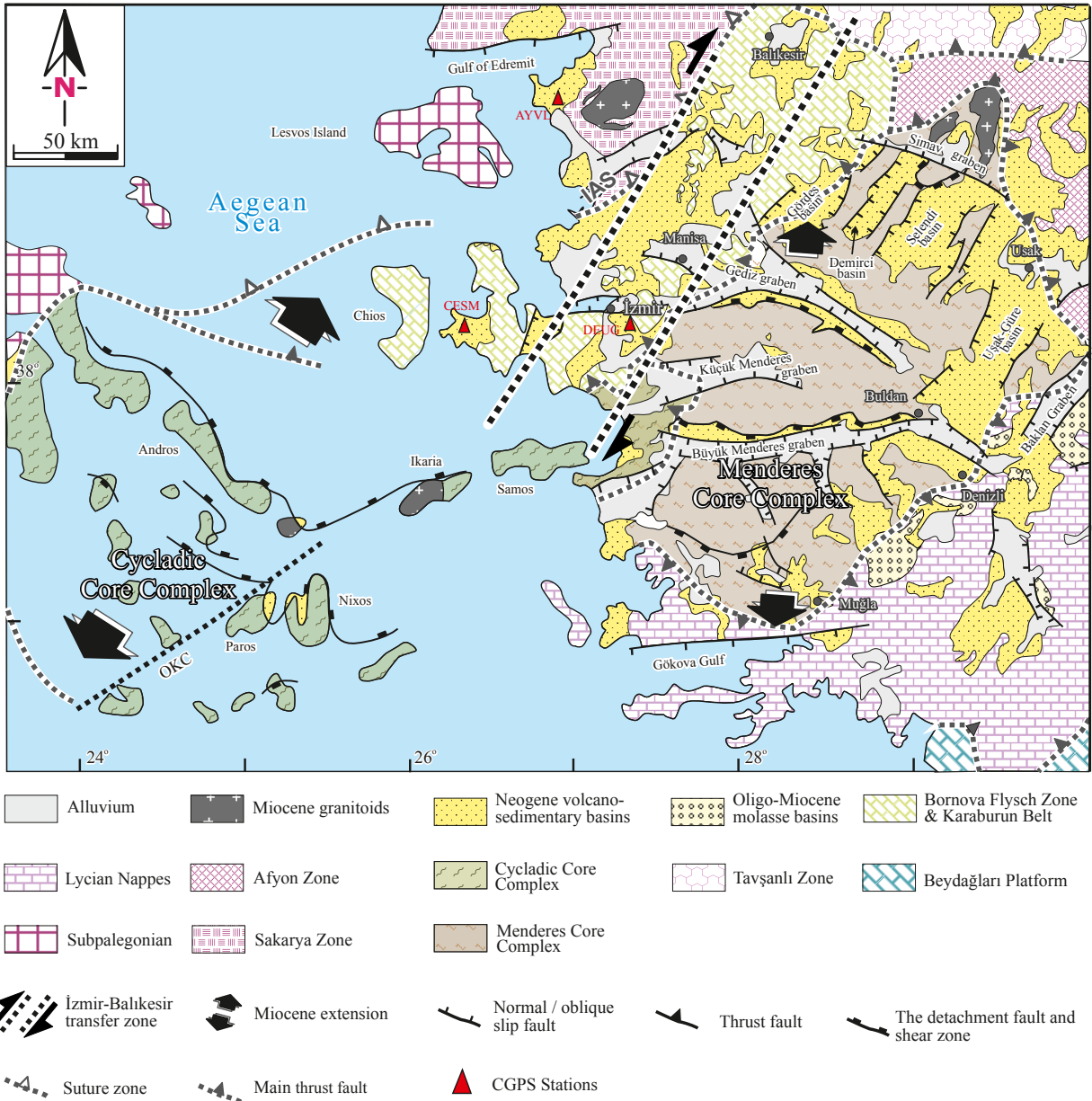
Figure 17. The horizontal displacements computed by Coulomb 3.3 software using the focal plane solutions of USGS (Table 4).

Table 4. Source parameters used as input for the Coulomb 3.3 software.

The name of the instution	Fault top/ bottom (km)	$M_w$	Depth (km)	Strike (°)	Dip (°)	Rake (°)
USGS	8/16	6.3	12	114	57	-82
Papadimitriou et al. (2018)	9/17	6.3	13	122	40	-83
KOERI	16/24	6.2	20	117	41	-76
AFAD	12/20	6.2	16	114	43	-78

Table 5. The CGPS-based offset estimates and the horizontal displacements computed by Coulomb 3.3 software.

	AYVL		CESM		DEUG	
	North (cm)	East (cm)	North (cm)	East (cm)	North (cm)	East (cm)
CGPS-based offsets	0.6	0.3	-0.3	0.08	0	0
USGS	1.2	2.2	-0.22	-1.6	-0.03	-0.05
Papadimitriou et al. (2018)	1.2	1.7	-0.33	-1.9	-0.04	-0.006
KOERI	0.64	1.22	-0.16	-1.4	-0.02	-0.03
AFAD	0.74	1.3	-0.16	-1.4	-0.02	-0.04



**Figure 18.** The basic geological map of the study area and its surroundings (modified from Sözbilir et al., 2011). The red triangles represent the locations of the CGPS stations.

this transfer zone may affect the seismic behaviour and the regional kinematic structure differently. Additionally, considering the epicentre of the earthquake, AYVL is the closest station to the main shock and thus it is the most affected station and TNZB represents different movement character with respect to the other stations.

The coseismic crustal deformation detected in this study suggests that the 12th June 2017 offshore Karaburun-Lesvos Island earthquake, which occurred at the Lesvos fault between the southwest of Lesvos Island and offshore

Karaburun, seemed to transfer its stress to İzmir and its surrounding. Lesvos fault is a normal fault and contains lateral fault zones which elongate from offshore Northern İzmir to the land. The type of faulting explains the reason why the horizontal coseismic deformation is much larger than the vertical coseismic deformation.

Consequently, an integrated use of CGPS and strong motion accelerometer networks for the joint assessment of the crustal deformation would be recommended for the cost-effective use of existing observation networks as well

as for the establishment of future observation networks at lower cost for earthquake monitoring.

## 7. Conclusion

The EMD analysis suggests that AYVL and CESM CGPS stations are affected from the earthquake but the most affected station is AYVL, besides, DEUG is almost not affected by this earthquake. According to the accelerometer records TNZB SMS presents smaller amplitudes respect to AYVL and CESM SMSs. The results of these methods are found as consistent with each other. The horizontal displacements obtained from Coulomb 3.3 software for different institutions' source parameters are found similar. The offsets in CGPS time series and the modelled

horizontal displacements are consistent with each other except the east component of CESM station.

## Acknowledgment

The accelerometer data of the strong motion stations are downloaded from the website <https://depem.afad.gov.tr/istasyonlar?lang=en#> provided by Republic of Turkey Disaster & Emergency Management Authority Presidential of Earthquake Department (AFAD). Continuous GPS data and photographs of AYVL and CESM stations are provided through CORS-TR (Continuously Operating Reference Stations-Turkey) jointly operated by General Directorate of Mapping (GDM) and General Directorate of Land Registry and Cadastre.

## References

- Baykut S, Akgul T, Ergintav S (2009). EMD-based analysis and denoising of GPS data. In: 2009 IEEE 17th Signal Processing and Communications Applications Conference; Antalya, Turkey. pp. 644-647.
- Baykut S, Akgül T, İnan S, Seyis C (2010). Observation and removal of daily quasi-periodic components in soil radon data. *Radiation Measurements* 45(4):872-879.
- Briole P, Ganas A, Karastathis V, Elias, P, Mouzakiotis E et al. (2018). The June 12, 2017 M6.3 Lesvos offshore earthquake sequence (Aegean Sea, Greece): fault model and ground deformation from seismic and geodetic observations. In: EGU General Assembly Conference Abstracts; Vienna, Austria. p. 18189.
- Chatzipetros A, Kiratzi A, Sboras S, Zouros N, Pavlides S (2013). Active faulting in the north-eastern Aegean Sea Islands. *Tectonophysics* 597: 106-122.
- Günther R, Kappelmeyer O, Kronberg P (1977). Zur prospektion auf geothermale anomalien, erfahrungen einer modelluntersuchung in Polichnitos, Lesbos (Griechenland). *Geologische Rundschau* 66: 10-33 (in German).
- Herring TA, King RW, Floyd MA, McClusky SC (2015). Introduction to GAMIT/GLOBK, Release 10.6. Cambridge, MA, USA: Massachusetts Institute of Technology.
- Huang NE, Shen Z, Long SR, Wu MC, Shih HH et al. (1998). The empirical mode decomposition and the Hilbert spectrum for nonlinear and non-stationary time series analysis. *Proceedings of the Royal Society London Series A, Mathematical and Physical Sciences* 454: 903-995.
- Huang NE, Chern CC, Huang K, Salvino LW, Long SR et al. (2001). A new spectral representation of earthquake data: Hilbert spectral analysis of station TCU129, Chi-Chi, Taiwan, 21 September 1999. *Bulletin of the Seismological Society of America* 91: 1310-1338.
- Huang NE, Wu Z (2008). A review on Hilbert-Huang transform: method and its applications to geophysical studies. *Reviews of Geophysics* 46 (2): 1-23.
- Kiratzi A, Louvari E (2003). Focal mechanisms of shallow earthquakes in the Aegean Sea and the surrounding lands determined by waveform modelling: a new database. *Journal of Geodynamics* 36: 251-274.
- Koukouvelas IK, Aydin A (2002). Fault structure and related basins of the North Aegean Sea and its surroundings. *Tectonics* 21: 1046.
- Kramer SL (1996). *Geotechnical Earthquake Engineering*. New Jersey, USA: Prentice Hall.
- Kreemer C, Chamot-Rooke N (2004). Contemporary kinematics of the southern Aegean Sea and the Mediterranean Ridge. *Marine Geology* 209: 303-327.
- Mao A, Harrison CGA, Dixon TH (1999). Noise in GPS coordinate time series. *Journal of Geophysical Research* 104: 2797-2816.
- Mucciarelli M, Gallipoli MR (2001). A critical review of 10 years of microtremor HVSR technique. *Bolletino di Geofisica Teorica ed Applicata* 42 (3-4): 255-266.
- Nakamura Y (1989). A method for dynamic characteristics estimation of subsurface using microtremor on the ground surface. *Quarterly Report of Railway Technical Research Institute (RTRI)* 30 (1).
- Papadimitriou P, Kassaras I, Kaviris G, Tselentis GA, Voulgaris N et al. (2018). The 12th June 2017 Mw= 6.3 Lesvos earthquake from detailed seismological observations. *Journal of Geodynamics* 115: 23-42.
- Papanikolaou D, Alexandri M, Nomikou P (2006). Active faulting in the north Aegean basin. *Geological Society of America Special Paper* 409: 189-209.
- Papazachos CB, Kiratzi AA (1996). A detailed study of the active crustal deformation in the Aegean and surrounding area. *Tectonophysics* 253: 129-153.

- Pavlidis S, Tsapanos T, Zouros N, Sboras S, Koravos G et al. (2009). Using active fault data for assessing seismic hazard: a case study from NE Aegean Sea, Greece. In: Earthquake Geotechnical Engineering Satellite Conference XVIIth International Conference on Soil Mechanics and Geotechnical Engineering; Alexandria, Egypt. pp. 2-3.
- Rato RT, Ortigueira M, Batista A (2008). On the HHT, its problems, and some solutions. *Mechanical Systems and Signal Processing* 22: 1374-1394.
- Sözbilir H, Sarı B, Uzel B, Sümer Ö, Akkiraz S (2011). Tectonic implications of transtensional supradetachment basin development in an extension-parallel transfer zone: the Kocaçay Basin, western Anatolia, Turkey. *Basin Research* 23 (4): 423-448.
- Toda S, Stein RS, Sevilgen V, LinJ (2011). *Coulomb 3.3 Graphic-Rich Deformation and Stress-Change Software for Earthquake, Tectonic, and Volcano Research and Teaching - User Guide*. U.S. Geological Survey Open-File Report 1060.2011.
- Wessel P, Luis JF, Uieda L, Scharroo R, Wobbe F et al. (2019). *The Generic Mapping Tools Version 6*. *Geochemistry, Geophysics, Geosystems* 20: 5556-5564.
- Williams SDP, Bock Y, Fang P, Jamason P, Nikolaidis RM et al. (2004). Error analysis of continuous GPS position time series. *Journal of Geophysical Research* 109 (B03412).
- Zouros N, Pavlidis S, Soulakellis N, Chatzipetros A, Vasileiadou K et al. (2011). Using active fault studies for raising public awareness and sensitisation on seismic hazard: a case study from Lesvos Petrified Forest Geopark, NE Aegean Sea, Greece. *Geoheritage* 3 (4): 317-327.